EUROPEAN ORGANIZATION FOR NUCLEAR RESEARCH

CERN-EP/81-169
21 December 1981

FAST-BEAM LASER SPECTROSCOPY ON METASTABLE ATOMS APPLIED TO NEUTRON-DEFICIENT YTTERBIUM ISOTOPES

F. Buchinger[1], A.C. Mueller[2], B. Schinzler[3], K. Wendt[4]

Institut für Physik, Universität Mainz,
Fed. Rep. Germany

C. Ekström[4]

Department of Physics, Chalmers University of Technology
and University of Gothenburg, Sweden

W. Klempt and R. Neugart

CERN, Geneva, Switzerland
and
the ISOLDE Collaboration, CERN, Geneva, Switzerland

ABSTRACT

The efficient population of metastable ^3P states in charge-transfer neutralization of Yb^+ beams with Na and Cs has been exploited for studies of isotope shifts in the even neutron-deficient and stable Yb isotopes ($156 \leq A \leq 176$). In addition, measurements have been performed in the intercombination line (5556 Å) from the ground state, primarily to obtain hyperfine structures and isotope shifts for a number of odd isotopes ($161 \leq A \leq 169$). The competitive advantages of different atomic transitions for sensitive high-resolution spectroscopy are discussed.

Contribution to the 6th International Conference on
Fast Ion Beam Spectroscopy,

Quebec, 17-20 August 1981

(To be published in Nuclear Instruments and Methods)

Present address:

1) Massachusetts Institute of Technology, Cambridge, Mass., USA.
2) Laboratoire René Bernas du CSNSM, Orsay, France.
3) Gewerbeaufsichtsverwaltung Hessen, Kassel, Fed. Rep. Germany.
4) CERN, Geneva, Switzerland.

1. INTRODUCTION

Collinear fast-beam laser spectroscopy has greatly enlarged the possibilities of studying nuclear moments and radii via the hyperfine structure (hfs) and isotope shift (IS) of atomic transitions. This progress, characterized by the advance to isotopes far from stability of an increasing number of elements, is essentially due to the ideal combination of i) resolution, ii) sensitivity, and iii) versatility of the method especially suitable for use in connection with on-line isotope separators[1].

The spectral *resolution* in the absorption of monochromatic laser light by a sample of atoms is mainly determined by the distribution of velocity components along the laser beam (Doppler broadening). Here, the phase-space properties of accelerated beams offer outstanding conditions. Constant energy spread δE during acceleration to a final energy eU leads to the narrowed Doppler width,

$$\delta\nu_D = \nu_0 \frac{\delta E}{(2eUmc^2)^{\frac{1}{2}}} ,$$

along the direction of beam propagation. A proper design of the ion source ($\delta E \simeq 1$ eV) and a stable acceleration voltage in the 10 kV to 100 kV range will ensure that this width is well-matched to the natural line width of strong optical transitions ($\delta\nu_{nat} \simeq 10$ MHz). Since no velocity-selecting mechanism is applied, all atoms in the beam contribute to the absorption signal detected by fluorescence.

The final *sensitivity* depends essentially on the strength of the optical transition, which determines the number of excitations and fluorescence photons per unit path length, as well as the ratio between natural line width and Doppler width. Background from scattered laser light, collisional excitation and radioactivity, limits the signal-to-noise ratio. For the $6s^2\ ^1S_0 \rightarrow 6s6p\ ^1P_1$ resonance transition in Ba I (5536 Å), a practical sensitivity limit of a few times 10^4 atoms/s has been established in recent experiments[2].

This high sensitivity, together with the fact that beams from on-line isotope separators are convenient samples -- requiring no collection and re-evaporation -- contributes a great deal to the *versatility* of the method. In order to reach optical transitions accessible with cw dye lasers, it is often advantageous to neutralize the beam by charge exchange in a vapour cell. Most collinear beam experiments on singly charged ions circumvented the problem of UV excitation by using transitions from metastable states, populated in the ion source[3,4]. There, a disadvantage for high-sensitivity experiments is the low population of metastable states and the difficulty of controlling their formation.

On the other hand, metastable *atomic* states can be very efficiently populated in the charge-transfer process. In the reaction

$$A + B^+ \rightarrow A^+ + B + \Delta E \ ,$$

where A and B^+ refer to an atomic vapour and the ion beam, respectively, the final states of B are preferably formed with a small energy defect ΔE[5]. This behaviour was demonstrated in the early experiments on collinear-beam spectroscopy using various combinations of alkali elements in the beam and the vapour target[6]. The observed structure of optical resonances could be attributed to the energy-loss spectrum of the neutralization process, reflecting itself in the Doppler shift. States, populated in B, tend to be as much below the ionization limit as the ground state of the reaction partner A. Since alkali vapours are commonly used for neutralization, this is between 3.9 eV for Cs and 5.1 eV for Na, from where strong transitions in the visible usually lead to higher excited states.

This mechanism is well known for the efficient population of the 2s state in hydrogen and the production of metastable noble-gas beams[7,8]. It has recently been applied for exploratory studies of the Balmer-α line by collinear-beam spectroscopy[9]. More generally it gives access to elements with resonance lines in the UV beyond the reach of cw dye lasers. In other cases, the wider choice of transitions can help to achieve higher sensitivity or to complement the information on nuclear properties.

2. SPECTROSCOPY ON YTTERBIUM

We have used this new variant of fast-beam laser spectroscopy for systematic investigations of the hfs and IS in the neutron-deficient Yb isotopes, covering the interesting transitional region between spherical and strongly deformed nuclear shapes above the N = 82 neutron shell closure. The 60 keV beams at ISOLDE[10] are extracted from a surface ionization source, connected to a Ta powder target (120 g/cm^2) at 2000 °C irradiated with 2 μA beams of 600 MeV protons. Yields of the spallation process ^{181}Ta(p,4p+xn)$^{178-x}$Yb are given in fig. 1. Beams of stable isotopes are obtained by loading the ion source with metallic Yb. The experimental set-up and its connection to the on-line isotope separator are described in refs. 1 and 2.

2.1 Sensitivity considerations and test experiments

The Yb spectrum (Fig. 2) represents an instructive example for sensitivity considerations and their relevance to the planning of the experiment. As in the alkaline earths, there is a strong transition from the $^1S_0$ ground state to the first excited $^1P_1$ state, which should be the most favourable candidate for high-sensitivity measurements similar to those reported for barium[2]. Unfortunately, the wavelength of 3988 Å is just beyond the reach of present single-mode dye lasers, whereas the weak intercombination line $^1S_0 \rightarrow {}^3P_1$ at 5556 Å has been one of the standard examples of high-resolution spectroscopy with lasers[11]. However, the long lifetimes of the $^3P_1$ state, τ = 875(20) ns [12], implies several disadvantages. During this time, an Yb atom in the 60 keV beam travels about 20 cm, which is the length of our observation region. Consequently, less than one spontaneous photon per atom is emitted on the average. Furthermore, the natural line width of 182(4) kHz is small compared to the Doppler width of 15 MHz, arising from the typical energy spread of the ion source and beam divergence. As a consequence, only about 1% of the atoms can absorb the narrow-band laser radiation -- unless the transition is power-broadened, which, on the other hand, increases the crucial background due to stray light. As a result, the limit of sensitivity can be expected at some 10^7 atoms/s, about three orders of magnitude above the weakest beam intensities used in the barium experiment[2].

What can be gained in transitions from metastable states? In fig. 2 we have indicated the ground-state energies of Na (-5.14 eV) and Cs (-3.89 eV), near which the maximum population of final states after charge exchange is expected. Neutralization with Cs should preferably lead to the ^3P states, of which $^3P_0$ and $^3P_2$ are metastable, whereas $^3P_1$ decays to the ground state as discussed above. Photons from this decay can be detected downstream in the observation region. From the intensity, using the known lifetime and photon-collection efficiency, we conclude that about 20% of the atoms are formed in the $^3P_1$ state. No significant difference between Na and Cs as reaction partners is found. This indicates that the energy-resonance condition is less pronounced at the relatively high beam energy of 60 keV. A population of the lowest s^2 and sp states according to their statistical weights seems to be a reasonable assumption, further confirmed by the observed fluorescence intensities for $^1S_0$ and $^3P_2$ excitation (see below).

Additional information on the final-state distribution in charge-exchange reactions can be obtained by resolving the velocity components of the beam[6]. Due to the Doppler shift, the line structure for $^1S_0$-$^3P_1$ resonance absorption can be interpreted in terms of the energy balance for the population of different atomic states (fig. 3). This structure is barely resolved, but a natural interpretation is consistent with the previous arguments: The main peak corresponds to atoms formed in the $^1P_1$ and $^3P_1$ states and decaying to the ground state before being excited by the laser light, whereas atoms formed directly in the ground state give rise to a small satellite peak at higher beam energy. The tail towards higher beam energies corresponds to the formation of higher excited states and secondary collisional processes. The metastable $^3P_0$ and $^3P_2$ states give no contribution, but can be assumed to be populated correspondingly.

These metastable states are connected to a number of ^3S and ^3D states by transitions at comfortable laser wavelengths. Favourite candidates for hfs and IS studies -- with the aim of measuring nuclear parameters -- are those involving the ^3S states. They involve a $p \rightarrow s$ transition of the valence electron and thus have a large field-shift contribution to the measured IS. We have not considered the transitions from the $^3P_0$ state because of its low statistical weight. For the remaining possibilities,

a) $6s6p\ ^3P_2 \rightarrow 6s7s\ ^3S_1$ (7699 Å),

b) $6s6p\ ^3P_2 \rightarrow 6s8s\ ^3S_1$ (4564 Å),

the high transition probability in the far-red line 7699 Å and the high detection efficiency in the weaker blue line 4564 Å represent competitive advantages.

The results of test experiments with both lines clearly favour the red one. The high transition rate at low laser power, and consequently low stray-light background, together with the shorter-wavelength decay channels (6800 Å, 6489 Å, 5556 Å), overcompensates the disadvantage of lower detection efficiency.

If we define the experimental sensitivity limit by the number of particles per second required to obtain a signal-to-noise ratio of 3 within 10 seconds, we can expect to perform a complete IS measurement within about one hour. These limits amount to 1×10^6 atoms/s and 2×10^7 atoms/s for cases (a) and (b), to be compared with 1×10^7 atoms/s for the intercombination line from the ground state.

2.2 Measurements on radioactive isotopes

For measurements on radioactive isotopes, additional considerations have to take into account the time limitations of accelerator experiments. We have to distinguish between the even-A isotopes with spin I = 0 and no hfs in any chosen transition, and the odd-A isotopes with a more or less complicated hfs pattern. The preference for pure IS measurements in the even isotopes should be given to the transition $6s6p\ ^3P_2 \rightarrow 6s7s\ ^3S_1$, ensuring the highest sensitivity. In the odd isotopes, this line has 9(8,3) hfs components for $I \geq 5/2$ ($I = 3/2, 1/2$), compared to 3(2) components for $I \geq 3/2$ ($I = 1/2$) in the intercombination line $6s^2\ ^1S_0 \rightarrow$ $\rightarrow 6s6p\ ^3P_1$. In the former case a measurement is complicated not only by the number of components which have to be found and assigned but also by the distribution of line strength over more components, counteracting the gain in sensitivity.

Therefore we adopted the strategy

i) of measuring the IS of the I = 0 isotopes as completely as possible in the 7699 Å transition from the metastable state, using the dye Oxazine 1;

ii) of continuing (after changing to Rhodamine 110), with measurements in the intercombination line 5556 Å, primarily on odd isotopes. Some of the high-yield even isotopes have to be included for a calibration of IS parameters by a King plot, via this well-investigated transition.

In a running period of two days, results were obtained on the even isotopes in the range $156 \leq A \leq 176$ for the red line 7699 Å, and on all isotopes in the range $A = 158$, $160 \leq A \leq 171$, for the intercombination line 5556 Å. For the latter, high-precision laser experiments on all stable isotopes had been performed previously by Clark et al.[11]. Champeau et al.[13] had investigated the long-lived radioactive isotope ^{169}Yb using conventional spectroscopy on a hollow-cathode discharge. Their results[11,13] are used in the following to complement the data, and to compare the results of overlapping measurements. The example of a measured spectrum for ^{156}Yb with the ^{168}Yb and ^{170}Yb reference spectra is shown in fig. 4.

The results are compiled in tables 1 and 2. Figure 5 gives the positions of all observed transitions in a frequency scale, relative to the lightest stable isotope ^{168}Yb. The perfect consistency of these results has been demonstrated in a King plot. This comparison between the two transitions used in the experiment indicates that the difference in specific mass shift contributions is small. The ratio of field shifts between $6s6p\ ^3P_2 \rightarrow 6s7s\ ^3S_1$ and $6s^2\ ^1S_0 \rightarrow 6s6p\ ^3P_1$ amounts to -0.4050(4).

In the lighter rare-earth elements, a sharp increase of the IS is observed between the neutron numbers $N = 88$ and $N = 90$, corresponding to an abrupt onset of nuclear deformation[14]. The present data for Yb, however, show a completely smooth behaviour, indicating a gradual increase of deformation between the $N = 82$ neutron shell closure and the strongly deformed stable isotopes. The evaluation of nuclear parameters (i.e. magnetic dipole and electric quadrupole moments) as well as the change of nuclear mean-square radii along the Yb chain will be discussed in a future publication, also devoted to the nuclear-physics interpretation. Very recently we have extended these studies to the neighbouring even-Z elements Er and Dy.

3. CONCLUDING REMARKS

We have shown that metastable atomic states, efficiently populated in charge-transfer collisions, can be favourably used in collinear-beam spectroscopy, and in particular for application to radioactive isotopes far from stability.

This scheme is certainly most valuable for elements with low-lying ground states and UV resonance lines. Test experiments have been successful with radioactive Hg isotopes, where the corresponding transition from the 6s6p $^3P_2$ metastable state (5461 Å) can be used to complete and improve the results obtained by RADOP [15] and pulsed-laser spectroscopy in the UV [16]. We would also like to draw attention to the interesting case of noble gases, where the population of the metastable $ns[3/2]_2$ states opens up the way to sensitive high-resolution experiments.

The experimental concept presented here can also be understood as a simplification of the well-established scheme of stepwise excitation[17], in so far as the first step is replaced by charge transfer into metastable states. Since the preferably populated states are close in energy to the alkali ground states, they can usually be further excited by cw laser light.

We would like to thank E.W. Otten for his advice and continuous encouragement. This work was supported in part by the Deutsche Forschungsgemeinschaft and the Bundesministerium für Forschung und Technologie.

REFERENCES

1) R. Neugart, Nucl. Instrum. Methods 186 (1981) 165, and references quoted therein.

2) A.C. Mueller, F. Buchinger, W. Klempt, E.W. Otten, C. Ekström, J. Heinemeier and R. Neugart, Spins, moments and charge radii of barium isotopes in the range $^{122-146}$Ba determined by collinear fast-beam laser spectroscopy, in preparation.

3) T. Meier, H. Hühnermann and H. Wagner, Opt. Commun. 20 (1977) 397.

4) R.E. Silverans, G. Borghs, G. Dumont and J.M. van den Cruyce, Z. Phys. A295 (1980) 311.

5) D. Rapp and W.E. Francis, J. Chem. Phys. 37 (1962) 2631.

6) K.-R. Anton, S.L. Kaufman, W. Klempt, G. Morruzzi, R. Neugart, E.W. Otten and B. Schinzler, Phys. Rev. Lett. 40 (1978) 642.

7) B.L. Donnally, T. Clapp, W. Sawyer and M. Schultz, Phys. Rev. Lett. 12 (1964) 502.

8) G.E. Ice and R.E. Olson, Phys. Rev. A11 (1975) 111.

9) E. Arnold, T. Kühl, E.W. Otten and L.v. Reisky, Collinear laser spectroscopy of the Balmer-α line, to be published in Opt. Commun.

10) H.L. Ravn, Phys. Rep. 54 (1979) 201.

11) D.L. Clark, M.E. Cage, D.A. Lewis and G.W. Greenlees, Phys. Rev. A20 (1979) 239.

12) M. Gustavsson, H. Lundberg, L. Nilsson and S. Svanberg. J. Opt. Soc. Am. 69 (1979) 984.

13) R.J. Champeau, J.J. Michel and H. Walther, J. Phys. B7 (1974) L262.

14) P. Brix and H. Kopfermann, Z. Phys. 126 (1949) 344.

15) J. Bonn, G. Huber, H.J. Kluge and E.W. Otten, Z. Phys. A276 (1976) 203.

16) P. Dabkiewicz, C. Duke, H. Fischer, T. Kühl, H.J. Kluge, H. Kremmling, E.W. Otten and H. Schüssler, J. Phys. Soc. Jap. 44 (1978) Suppl. 503.

17) V.I. Balykin, G.I. Bekov, V.S. Letokhov and V.I. Mishin, Sov. Phys.- Usp. 23 (1980) 651.

Table 1

Isotopes shifts for the Yb I lines 7699 Å and 5556 Å, with respect to ^{168}Yb. The present collinear-beam results are calculated from Doppler shifts using atomic masses according to Wapstra and Bos[a]. The errors include systematic uncertainties of the voltage calibration and mass values, as well as statistical errors of the line positions.

Isotope A	$\delta\nu^{168,A}$ (MHz)	
	7699Å	5556 Å
156	-5794(10)	
158	-4696(6)	11220(12)
160	-3605(6)	8601(10)
161	-	7605(8)
162	-2538(6)	6053(8)
163	-	5094(7)
164	-1548(5)	3675(6)
165	-	2823(3)
166	-691.2(1.5)	1634(4)
167	-	756(8)
168	0	0
169	-	-611(3) -602(14) [b]
170	582.4(1.3)	-1369.9(1.6) -1368.63(50) [c]
171	-	-1829(3) -1829.33(50) [c]
172	1130(5)	-2655.10(50) [c]
173	-	-3099.76(50) [c]
174	1562(5)	-3655.38(50) [c]
176	1978(6)	-4610.14(50) [c]

a) A.H. Wapstra and K. Bos, Atomic Data and Nuclear Data tables 19 (1977) 177.
b) Champeau et al. (Ref. 13).
c) Clark et al. (Ref. 11).

Table 2

Magnetic dipole and electric quadrupole coupling constants in the $6s6p\ ^3P_1$ state from the hfs of the Yb I line 5556 Å. The spin assignments for $^{161-167}Yb$ have been made on the basis of the intensity ratios of the hyperfine components. They are supported by the close agreement between the experimental hfs and that predicted from the nuclear moments of lighter isotones.

Isotope	I	A (MHz)	B (MHz)
161	3/2	-878(3)	-303.2(1.9)
163	3/2	-1003(3)	-367.1(1.9)
165	5/2	769.1(1.1)	-732(4)
167	5/2	1000(4)	-786(14)
169	7/2	-730.2(0.8) -728(10) a)	-1045(5) -1038(15) a)
171	1/2	3955(4) 3957.97(47) b)	0
173	5/2	-1094.20(60) b)	-827.15(47) b)

a) Champeau et al. (Ref. 13)

b) Clark et al. (Ref. 11).

Figure captions

Fig. 1 : Production yield of Yb isotopes from the ISOLDE separator. Nuclides studied in this work are represented by full circles.

Fig. 2 : Partial energy-level diagram for Yb I, including the levels and transitions discussed in the text. The ground-state energies of Cs (-3.89 eV) and Na (-5.14 eV) relative to the ionization limit are also indicated.

Fig. 3 : Resonance curve corresponding to the $6s^2\ ^1S_0 \rightarrow 6s6p\ ^3P_1$ transition in ^{174}Yb. The relative positions of velocity components, arising from charge transfer into different final states, are indicated at the bottom. The FWHM corresponds to 12 MHz in a frequency scale.

Fig. 4 : Resonances recorded in the 7699 Å line in a measurement on ^{156}Yb, with ^{168}Yb and ^{170}Yb as reference isotopes. The total measuring time was about 30 min and the FWHM corresponds to 33 MHz.

Fig. 5 : Positions of the hfs components and the centres of gravity in the 5556 Å and 7699 Å lines for $^{156-176}$Yb, with respect to ^{168}Yb. Data for the stable isotopes in the 5556 Å line are taken from Clark et al.[11]. Nuclear spin values are given on the top and the hfs components are denoted by the quantum number F.

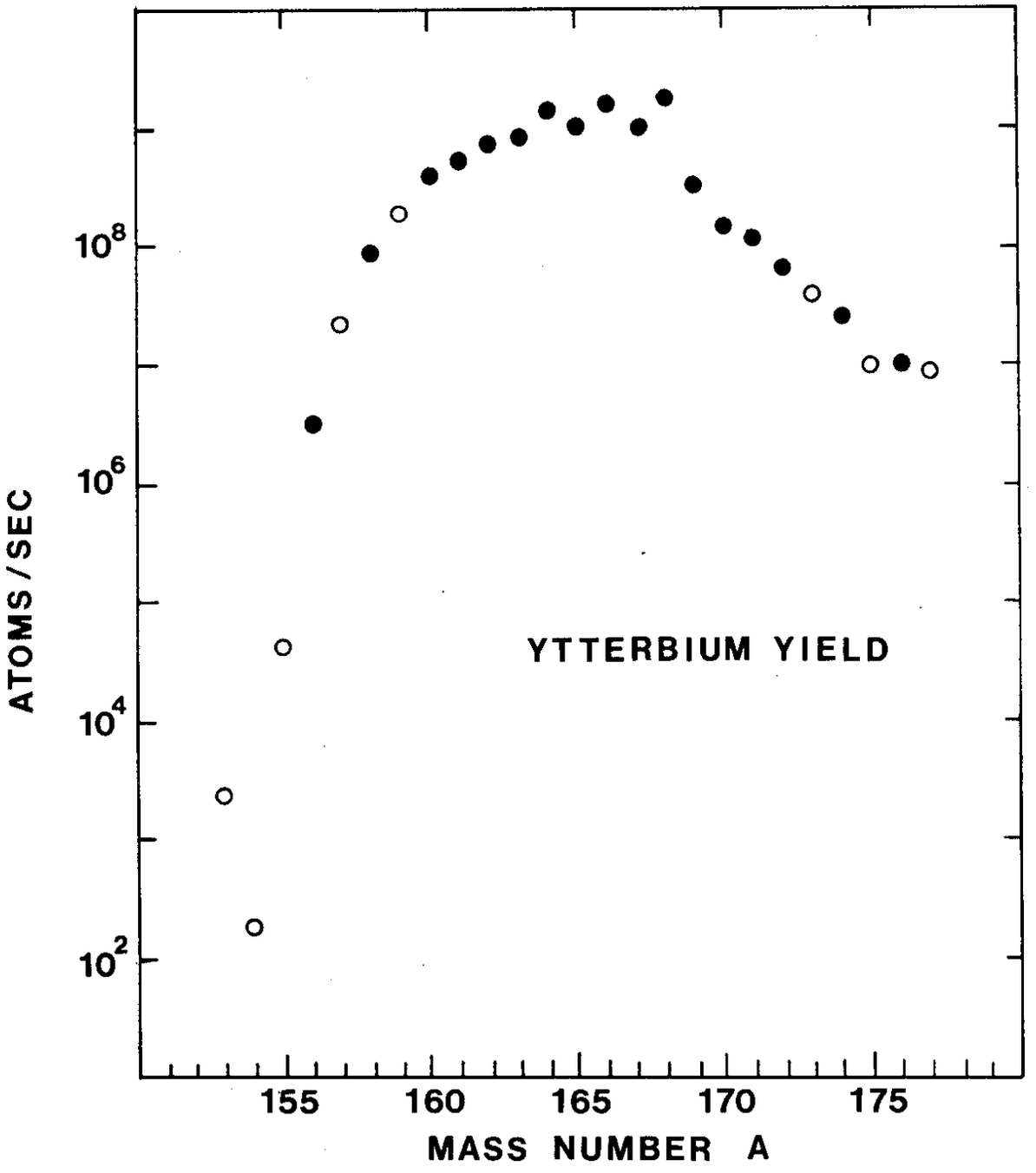
ATOMS/SEC
10^8
10^6
10^4
10^2
YTTERBIUM YIELD
155
160
165
170
175
MASS NUMBER A

Fig. 1

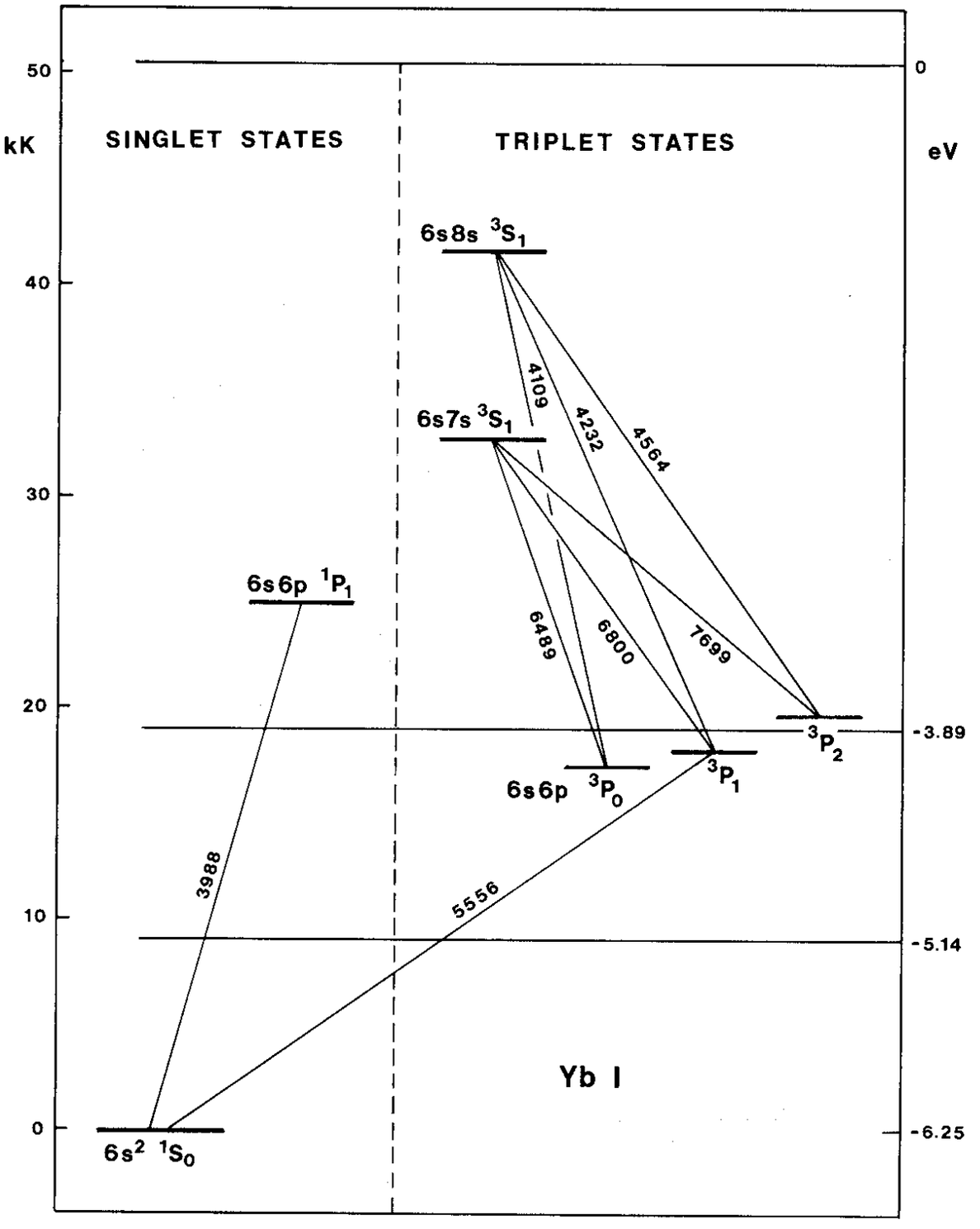
50
40
30
20
10
0
kK
SINGLET STATES
TRIPLET STATES
0
eV
-3.89
-5.14
-6.25
6s8s $^3S_1$
6s7s $^3S_1$
6s6p $^1P_1$
6s6p $^3P_0$
$^3P_1$
$^3P_2$
6s^2 $^1S_0$
4109
4232
4564
6489
6800
7699
3988
5556
Yb I

Fig. 2

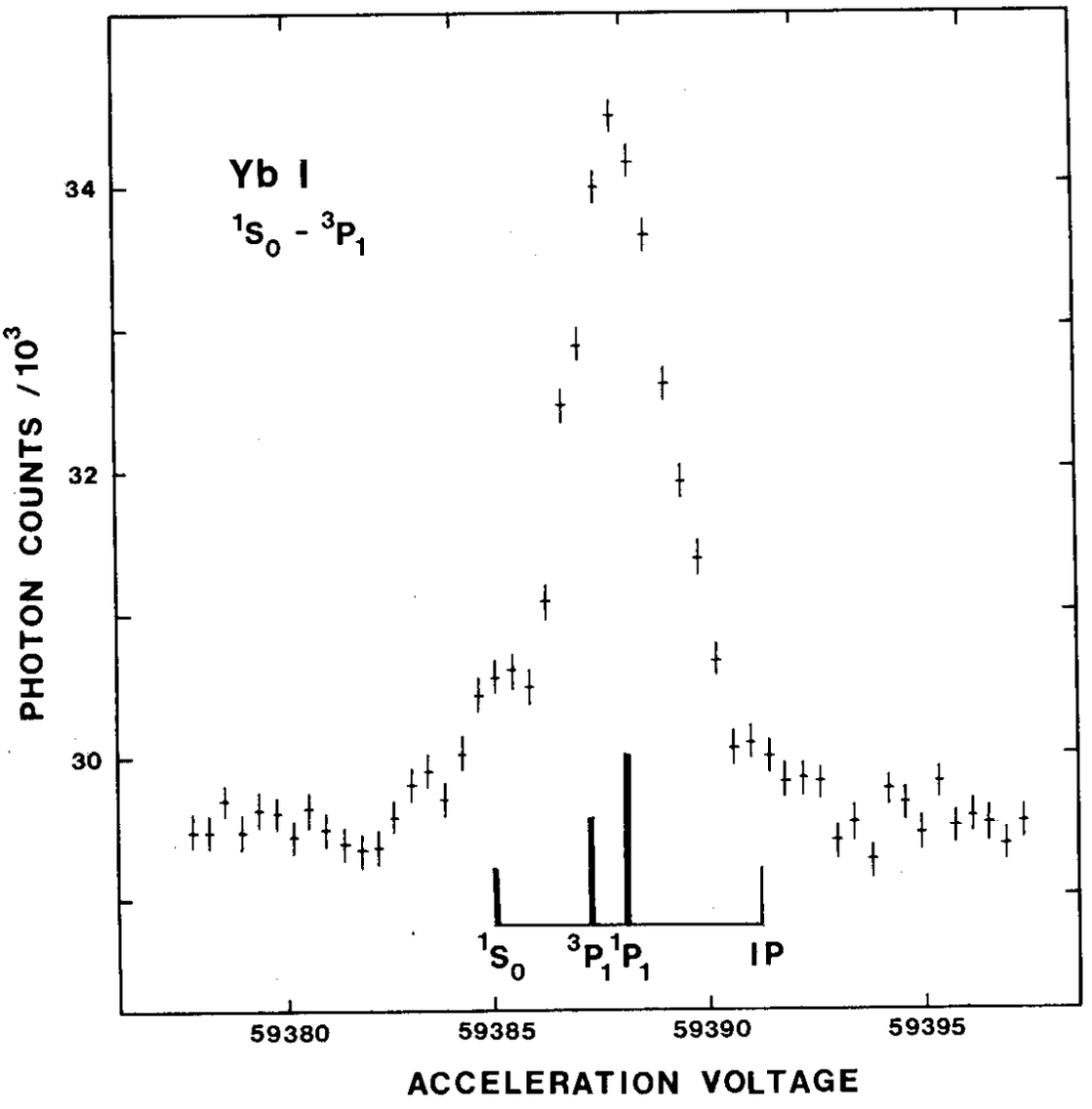
Yb I
$^1S_0$ - $^3P_1$
PHOTON COUNTS /10^3
34
32
30
59380
59385
59390
59395
ACCELERATION VOLTAGE
$^1S_0$
$^3P_1$ $^1P_1$
IP

Fig. 3

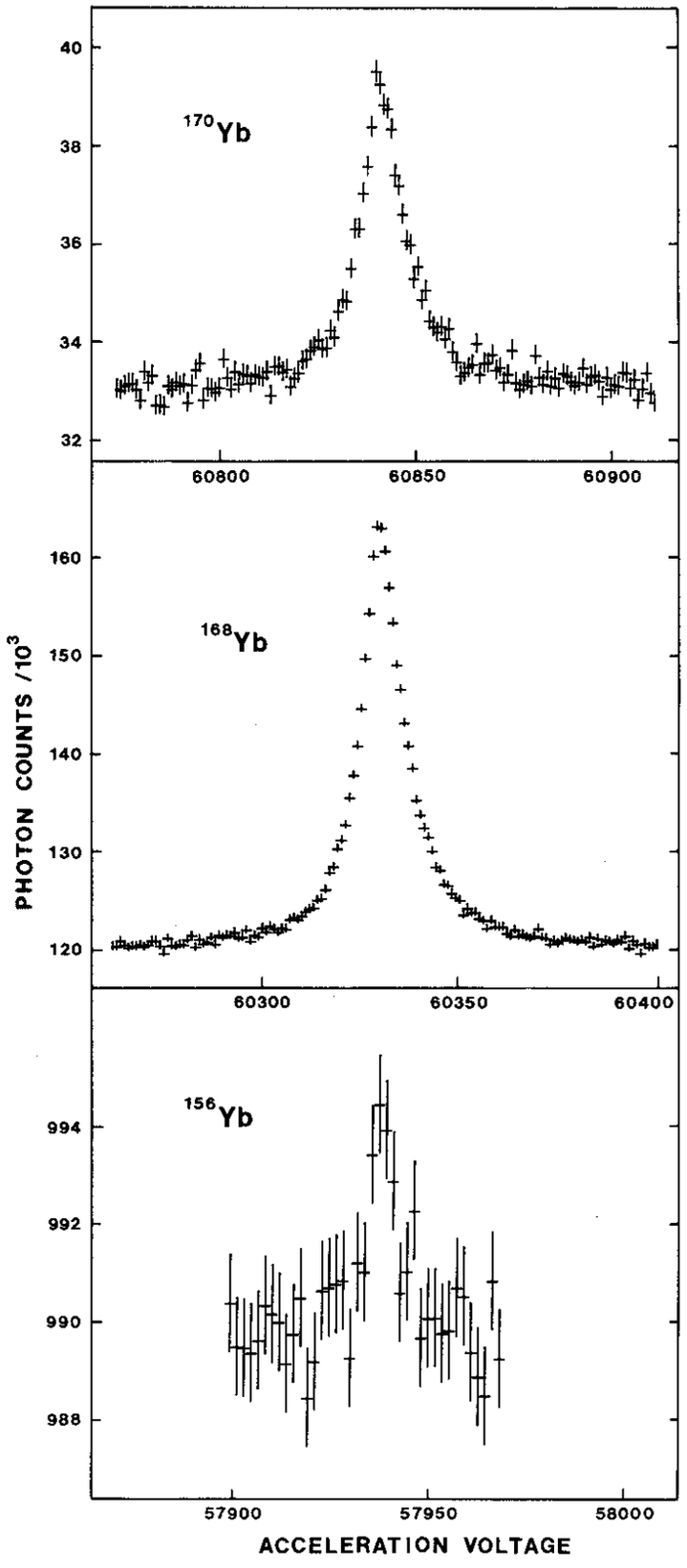
^{170}Yb
^{168}Yb
^{156}Yb
PHOTON COUNTS /10^3
ACCELERATION VOLTAGE
40
38
36
34
32
60800
60850
60900
160
150
140
130
120
60300
60350
60400
994
992
990
988
57900
57950
58000

Fig. 4

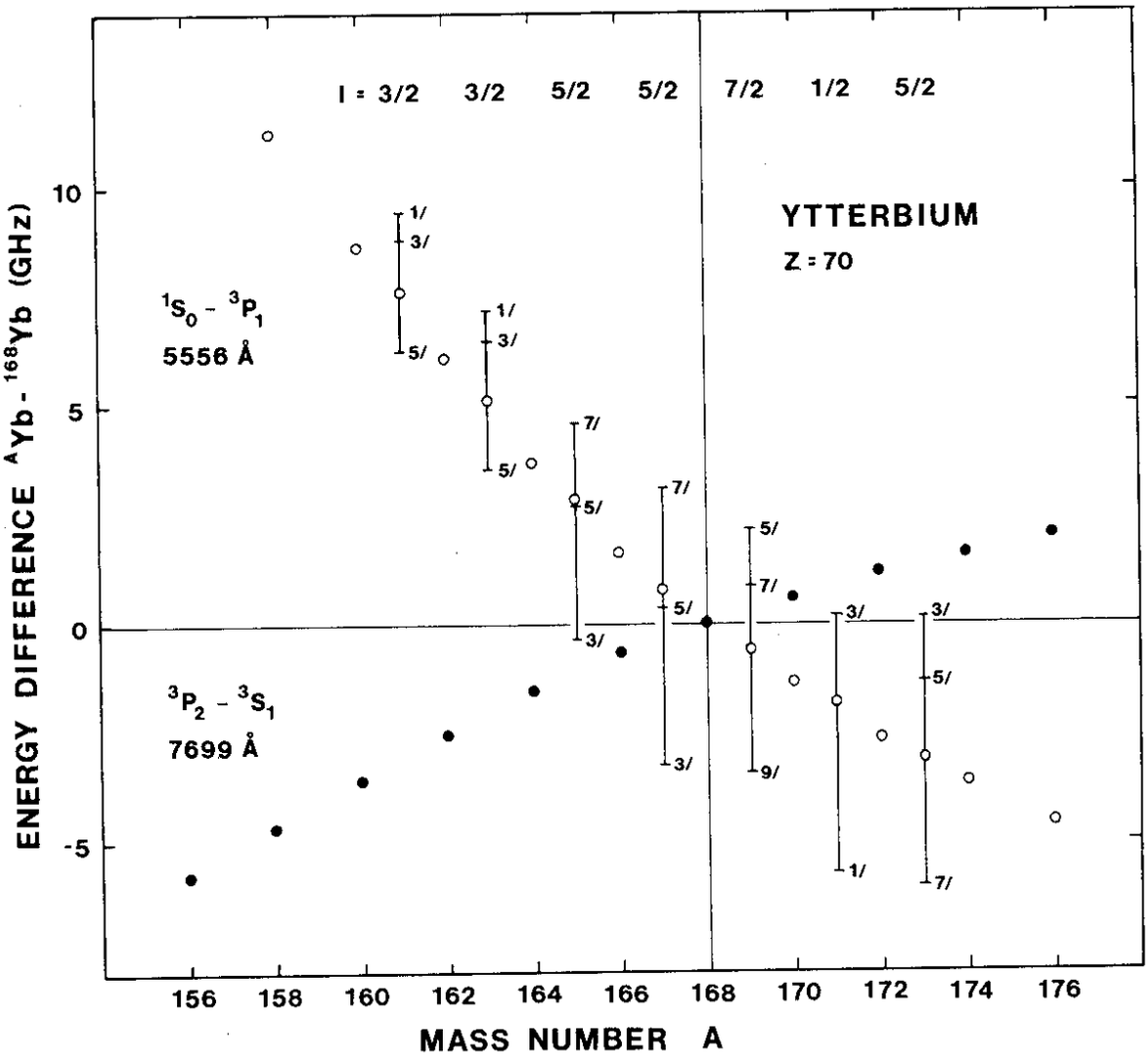
I = 3/2 3/2 5/2 5/2 7/2 1/2 5/2
YTTERBIUM
Z = 70
$^1S_0 - {}^3P_1$
5556 Å
$^3P_2 - {}^3S_1$
7699 Å
ENERGY DIFFERENCE ^{A}Yb - ^{168}Yb (GHz)
MASS NUMBER A
10
5
0
-5
156 158 160 162 164 166 168 170 172 174 176
1/
3/
5/
7/
9/

Fig. 5